Lifetime Broadening in the Rotationally Resolved Electronic Spectra of Dibenzothiophene, 2,5-Diphenylfuran, and 2,5-Diphenyl-1,3,4-oxadiazole in the Gas Phase. Intersystem Crossing Dynamics in the Statistical Limit.

Leonardo Alvarez-Valtierra,[†] John T. Yi,[‡] and David W. Pratt*

Department of Chemistry, University of Pittsburgh, Pittsburgh, Pennsylvania 15260

Received: August 18, 2008; Revised Manuscript Received: November 03, 2008

The fluorescence lifetime of the zero point vibrational level of the first excited electronic state of dibenzothiophene (DBT) has been determined to be 1.0 ns by analysis of its rotationally resolved $S_1 \leftarrow S_0$ fluorescence excitation spectrum. The S_1 lifetime of DBT is substantially shorter than those observed for fluorene (FLU), carbazole (CAR), and dibenzofuran (DBF), analogs of DBT in which the heavy sulfur atom is replaced by lighter ones. The electronic origin bands through the series CAR, FLU, DBF, and DBT exhibit a monotonic increase in Lorentzian broadening in their Voigt line shape profiles. Two other heterocyclic molecules manifest similar photophysical properties; 2,5-diphenylfuran and 2,5-diphenyl-1,3,4-oxadiazole. Lorentzian line shape broadenings of $\sim$ 76 MHz were observed in the high-resolution spectra of their origin bands. Possible reasons for the short fluorescence lifetimes of these heterocycles are discussed.

1. Introduction

A radiationless transition is a change in the electronic state of a molecule that occurs without the absorption or emission of radiation. Radiationless transitions are transfers of energy from one part of a multidimensional potential energy surface to another, and therefore are related to all types of chemical transformations. The various types of nonradiative transitions in vibrationally and/or electronically excited molecules, such as intramolecular vibrational relaxation (IVR), internal conversion (IC), and intersystem crossing (ISC), are usually described by two sets of zero-order levels: a bright state $|s\rangle$ that carries the oscillator strength and a bath of nearly isoenergetic dark states $\{|t\rangle\}$ to which the bright state is coupled (see Figure 1). The decay behavior of the prepared state depends upon the energy level density ρ_t, the full width at half-maximum (FWHM) decay widths γ_t, and the $|s\rangle - \{|t\rangle\}$ coupling terms k_{st}. Using the molecular limit classification scheme first proposed by Robinson[1] for the different types of decay behavior of chemical systems, we focus here on the large molecule (statistical) limit; i.e., $x_t = \rho_t\gamma_t \gg 1$. In this limit, the average level spacing ε_t is small, there are a large number of couplings between the two manifolds, and the oscillator strength is spread out over a large number of levels. If only a fraction of these are contained within the excitation bandwidth, then the initial state decays exponentially with a rate that is faster than the radiative rate, and the emission quantum yield is low.

Some heterocyclic aromatic molecules are known to exhibit fascinating photophysical properties in terms of ISC dynamics, in the large molecule limit, upon electronic excitation with monochromatic light.[2] Dibenzothiophene (DBT) is an excellent example. Pioneering spectroscopic studies of DBT were performed by analyzing its electronic absorption spectra in crystal lattices.[3−5] The orientations of the electronic transition moment vectors were determined for different electronic states.[4,5] Additionally, the transition energies, band polarizations, and dipole strengths of DBT, carbazole (CAR), and dibenzofuran (DBF) were measured in the condensed phase by UV linear and magnetic circular dichroism.[6,7] Important findings in terms of the effects of heavy atoms, planarity and rigidity of heterocyclic molecules on their photophysical properties, and ISC rates have recently been reported.[8−10] Zander and Kirsch[8] have found that the fluorescence quantum yield decreases by a factor of 16 upon substitution of the oxygen atom in DBF by sulfur to form DBT. Nijegorodov and co-workers[10] have shown that the change in fluorescence quantum yield in the series FLU-CAR-DBF-DBT (FLU = fluorene) can be entirely attributed to the internal heavy atom effect in the condensed phase experiments. This observation suggests a considerable increase in the ISC rate constant k_{st} due to increases in the magnitude of the spin−orbit coupling operator in the molecular Hamiltonian and in the degree of conjugation of the heteroatom's electron lone-pairs with the

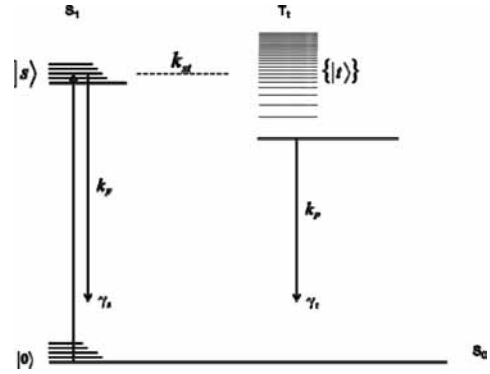

Figure 1. Radiationless transitions in a large molecule. $|s\rangle$ denotes the bright state that is optically prepared by excitation of the ground state $|0\rangle$, and coupled via matrix elements k_{st} to a dense manifold of nearly isoenergetic dark states $\{|t\rangle\}$. In ISC, S_1 and T_t are zero-order singlet and triplet states, respectively, and k_{st} is its interaction rate constant. k_F and k_P are the fluorescence and phosphorescence rate constants, whereas γ_s and γ_t are the radiative and nonradiative decay widths, respectively.

* Corresponding author. E-mail: pratt@pitt.edu.
[†] Current address: Instituto de Ciencias Físicas, Universidad Nacional Autónoma de México, Cuernavaca, Mor. 62210, México.
[‡] Current address: Department of Chemistry, Winston-Salem State University, Winston-Salem, NC 27103.

10.1021/jp807397t CCC: $40.75 © 2009 American Chemical Society
Published on Web 02/16/2009

π-electron cloud. Thus, replacement of carbon atoms by either oxygen or sulfur nearly always red-shifts the fluorescence excitation frequency, lowers the fluorescence quantum yield, and increases k_{st} in electronic excitation.[11]

Interestingly, some either nitrogen- or oxygen-containing heterocycles also manifest different fluorescence and phosphorescence properties.[11,12] Heterocycles such as 2,5-diphenylfuran (DPF) and 2,5-diphenyl-1,3,4-oxadiazole (DPO) are known to exhibit (S_1-T_1) spin−orbit coupling, facilitating the ISC efficiency.[13−15] What is not known is how these molecules behave as isolated species in the gas phase.

In this work, we report the rotationally resolved $S_1 \leftarrow S_0$ fluorescence excitation spectra of DBT, DPF, and DPO in the collision-free environment of a molecular beam. These molecules lie in the statistical limit of ISC, and therefore exhibit anomalous Lorentzian (lifetime) broadening in their rotational transitions, from which their fluorescence lifetime can be determined. This makes possible an examination of the trends in ISC dynamics exhibited by the entire family of molecules.

2. Experimental Section

DBT, DPF, and DPO (>98% pure) were purchased from Aldrich and used without further purification. Either dry helium or argon was used as an inert carrier gas for our experiments.

In the vibrationally resolved experiments, samples were seeded into 55 psi of helium gas (for DBT) and 20 psi of argon gas (for DPF and DPO) and expanded into a vacuum chamber (10^{-5} torr) through a 1 mm diameter orifice pulsed valve (General Valve Series 9) operating at 10 Hz. Two centimeters downstream of the valve, the free jet was excited with the second harmonic of a Quanta Ray Nd^{3+}:YAG (Model DCR-1A) pumped dye laser (Model PDL-1). The dye laser output (DCM for DBT and DPF, and Kiton Red 620 for DPO) was frequency doubled with an external KDP crystal providing a spectral resolution of $\sim$0.6 cm^{-1} in the UV. The molecules were excited at the point of intersection between the jet and the laser beam, and the resulting fluorescence was collected with a photomultiplier tube (PMT). Finally, the collected data were processed by a boxcar integrator (Stanford Research Systems) and recorded with Quick Data Acquisition software (Version 1.0.5).

Rotationally resolved electronic experiments were performed using a molecular beam laser spectrometer, described in detail elsewhere.[16] Briefly, the molecular beam was formed by expansion of the vaporized samples seeded either in helium (−5 psi) or argon (−16 psi) through a heated ($\sim$395 K) 200 μm quartz nozzle into a differentially pumped vacuum system. The expansion was skimmed 2 cm downstream with a 1 mm diameter skimmer and crossed 13 cm further downstream by a continuous wave (CW) Ar^+ pumped ring dye laser. The CW laser was operated with either DCM or Rhodamine 6G dye and intracavity frequency doubled in either a 630 nm $LiIO_3$ or a 600 nm β-barium borate (BBO) crystal, yielding $\sim$250 μW of UV radiation with a resolution of $\sim$1 MHz. The fluorescence excitation spectra were detected, using spatially selective optics, by a PMT and a photon counting system. The PMT signal together with the iodine absorption spectrum and the relative frequency markers were simultaneously collected and processed by the JBA95 data acquisition system.[16] Absolute frequency calibration of the spectra was performed by comparison with the I_2 absorption spectrum. The relative frequency markers were obtained from a stabilized etalon with a free spectral range of 299.7520 ± 0.0005 MHz.

3. Results

Figure 2 shows the vibrationally resolved (low-resolution) fluorescence excitation spectra of FLU, CAR, DBF, and DBT in a supersonic jet. Similar scans of some of these spectra have been previously reported elsewhere.[17−20] However, the jet-cooled low-resolution laser-induced fluorescence (LIF) spectrum of DBT is presented here for the first time. Two relatively intense vibronic bands (marked in Figure 2) appear in the spectrum of DBT at 202 and 482 cm^{-1} above the origin band. These vibronic bands in DBT lie at frequencies similar to those previously observed in FLU, CAR, and DBF; some of these exhibit different band polarizations due to a Herzberg−Teller coupling mechanism involving the S_2 state.[20]

Figure 3 shows the rotationally resolved $S_1 \leftarrow S_0$ fluorescence excitation spectrum of the 0_0^0 band of DBT located at 31187.3 cm^{-1} (about 2588 cm^{-1} red-shifted from that of FLU[20]). It spans approximately 2.5 cm^{-1} and exhibits an overall broad bandwidth and pure *b*-type character. To fit this spectrum, we first generated $\sim$9000 rovibronic transitions based on ab initio estimates[21] of the S_0 rotational constants and rigid rotor Hamiltonians for both electronic states, using *b*-type selection rules. Then, we made quantum number assignments of single transitions in the simulated spectrum to corresponding transitions in the experimental spectrum, using the Windows-based program JB95.[22] Finally, we used a least-squares fitting procedure to optimize the rotational constants, based on a comparison of observed and calculated line positions. The final fit utilized 176 rovibronic transitions and resulted in a standard deviation (observed minus calculated (OMC)) of 3.5 MHz. The quality of this fit is shown in the bottom panel of Figure 3. Individual lines in the fit exhibit Voigt profiles, with a Gaussian line width of 18 MHz and a Lorentzian line width of 167 MHz. The rotational temperature of the fit is 9 K.

Similarly, the DBT+202 vibronic transition also has been recorded and fully analyzed. The rotationally resolved electronic spectrum of this band spans approximately 2.5 cm^{-1} and exhibits pure *b*-type rovibronic transitions. The Voigt profile used for the fit required 18 MHz Gaussian and 196 MHz Lorentzian contributions. The rotational temperature of the fit is 10 K. The inertial parameters of this band are reported in Table 1.

Figure 4 shows the corresponding low-resolution LIF spectra of DPF and DPO in the gas phase. The features observed in both spectra agree with the ones previously reported by Topp and co-workers.[23] The 0_0^0 band of DPF is red-shifted by 18087 and 3031 cm^{-1} with respect to the $\pi\pi^*$ origin bands of furan[24] and DBF,[20] respectively. The two most intense vibronic transitions have been found at 265 and 876 cm^{-1} away from the origin band. The 0_0^0 band of DPO, however, is $\sim$ 3000 cm^{-1} blue-shifted from that of DPF and exhibits more vibronic activity in the region near the origin, such as the +66 and the +254 cm^{-1} bands.

Figure 5 shows the rotationally resolved $S_1 \leftarrow S_0$ fluorescence excitation spectrum of the 0_0^0 band of DPF at 30613.3 cm^{-1}. It spans approximately 1.2 cm^{-1} and exhibits pure *a*-type character, revealing that the $S_1 \leftarrow S_0$ transition moment vector is oriented parallel to the *a*-inertial axis. A procedure similar from that used for DBT was used to fit this band. The final fit, using rigid rotor Hamiltonians, utilized $\sim$150 assigned transitions resulting in a standard deviation of 2.98 MHz. The rotational temperature of the fit is 4 K. The Voigt line shape profile required 18 MHz Gaussian and 75 MHz Lorentzian contributions. The quality of the fit is shown at the bottom of Figure 5, where a fully resolved portion of the experimental *P* branch is shown along with its simulated spectrum.

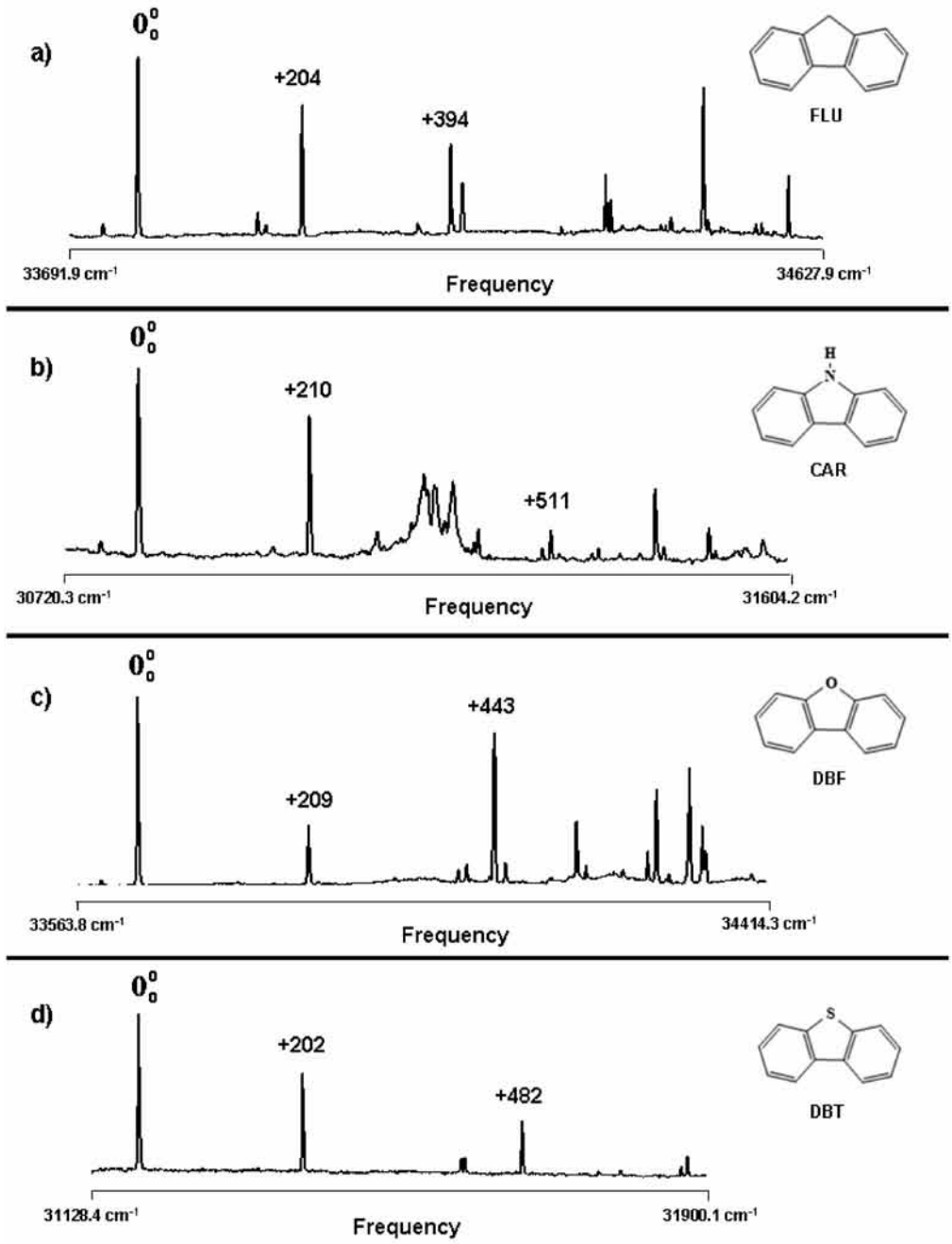

Figure 2. Vibrationally resolved fluorescence excitation spectra of FLU, CAR, DBF, and DBT in the gas phase.

Finally, Figure 6 shows the rotationally resolved $S_1 \leftarrow S_0$ fluorescence excitation spectrum of the 0_0^0 band of DPO in the gas phase. It spans approximately 1.3 cm^{-1} and also exhibits pure *a*-type character. To fit this spectrum, rigid rotor Hamiltonians were used for both electronic states. Approximately 130 simulated rovibronic transitions were assigned to the experimental spectrum, resulting in a standard deviation of 2.40 MHz. The rotational temperature of the fit is 5 K. The Voigt profile used 18 MHz Gaussian and 77 MHz Lorentzian contributions. The inertial parameters of the fits of these two bands are also reported in Table 1.

4. Discussion

Spectroscopy. The rotationally resolved $S_1 \leftarrow S_0$ fluorescence excitation spectra of FLU, CAR, and DBF in the gas phase have been recently analyzed.[20] This analysis shows that some of the higher lying vibronic bands exhibit anomalous polarizations, suggesting a Herzberg−Teller coupling of the S_1 state with the nearby S_2 state. Here, we analyze the lifetime (Lorentzian) broadening of single rovibronic transitions of the S_1-S_0 origin band in DBT, and contrast its behavior with those of its analogs (FLU, CAR, and DBF) in greater detail.

From the fit of the spectrum in Figure 3, we find that DBT exhibits a *b*-axis polarized $S_1 \leftarrow S_0$ electronic transition, in agreement with previous results in crystal lattices.[4,5] The S_1 state of isolated DBT is an ^1L_a state in the Platt perimeter model (see Figure 7a),[25] which means that its photochemical behavior is similar to that of CAR and DBF (^1L_a states), but very different from that of FLU (^1L_b state).[20]

The calculated ground-state rotational constants (MP2/6-31G**) of DBT are in excellent agreement with the experimental ones (cf. Table 1). In most aromatic molecules, excited state

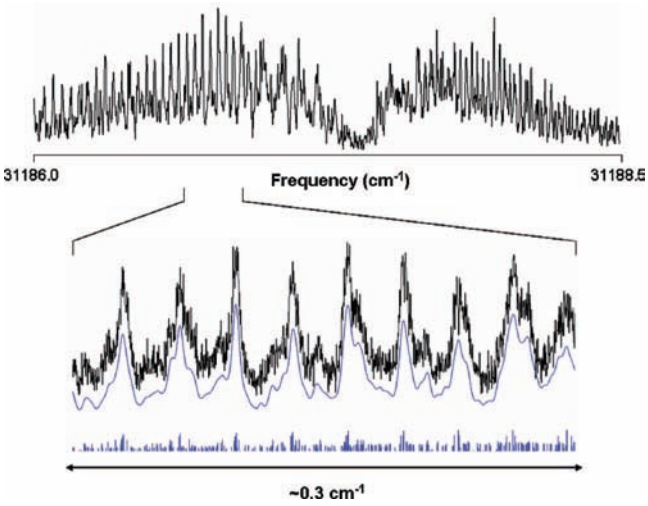

Figure 3. Rotationally resolved fluorescence excitation spectrum of the 0_0^0 band of DBT in the gas phase; the origin frequency is at 31187.3 cm^{-1}. A portion of the experimental trace and its corresponding simulated spectrum, with and without line shape functions, are also shown in the bottom panel.

TABLE 1: Inertial Parameters of the Origin Bands of DBT, DPF, and DPO in Their Ground and Excited Electronic States

parameter[a]	DBT[b]	DBT+202	DPF[c]	DPO[d]
S_0				
A'' (MHz)	1606.9 (1)	1606.0 (1)	1449.7 (1)	1619.7 (1)
B'' (MHz)	578.7 (1)	578.9 (1)	217.8 (1)	212.9 (1)
C'' (MHz)	425.7 (1)	425.8 (1)	189.2 (1)	187.9 (1)
$\Delta I''$ (uÅ^2)	−0.74 (5)	−0.75 (5)	1.86 (5)	3.35 (5)
S_1				
A' (MHz)	1628.1 (1)	1629.7 (1)	1456.5 (1)	1629.9 (1)
B' (MHz)	569.7 (1)	570.0 (1)	218.8 (1)	213.5 (1)
C' (MHz)	422.3 (1)	422.3 (1)	190.0 (1)	188.5 (1)
$\Delta I'$ (uÅ^2)	−0.73 (5)	0.00 (5)	3.22 (5)	4.10 (5)
band origin (cm^{-1})	31187.3	31389.3	30613.3	33695.9
OMC (MHz)	3.51	4.04	2.98	2.40
band type	*b*	*b*	*a*	*a*

[a] The standard deviations in the last significant figure are shown in parentheses. [b] MP2/6-31G** rotational constants: $A'' = 1597.4$ MHz, $B'' = 579.0$ MHz, $C'' = 425.0$ MHz. [c] MP2/6-31G** rotational constants: $A'' = 1420.5$ MHz, $B'' = 218.4$ MHz, $C'' = 189.3$ MHz. [d] MP2/6-31G** rotational constants: $A'' = 1610.1$ MHz, $B'' = 212.7$ MHz, $C'' = 187.9$ MHz.

A', B', and C' values are smaller in magnitude than their ground-state counterparts, owing to the small ring expansions that are typical of $\pi\pi^*$ states. However, in DBT, ΔA ($A' - A''$) is positive (21.2 MHz), whereas ΔB and ΔC are slightly negative (−9.0 and −3.4 MHz, respectively). Similar effects were observed in CAR and DBF.[20] All three molecules appear to contract in directions perpendicular to their *a*-axes when the photon is absorbed. In contrast, ΔA in FLU is large and negative, suggesting an expansion in directions perpendicular to its *a*-axis. There also is more delocalization of the lone pair electrons in CAR and DBT, compared to DBF and FLU, since their origin bands are red-shifted by relatively large amounts.

DBT is essentially planar in both electronic states. It has inertial defect values ($\Delta I = I_c - I_a - I_b$) of −0.74 uÅ^2 in its S_0 state and −0.73 uÅ^2 in its S_1 electronic state, values that are consistent with a planar molecule ($\Delta I \approx 0$). The values of ΔI do not seem to change substantially when the molecule absorbs light. Additionally, from the *b*-type selection rules employed to fit the origin band of DBT, the transition moment vector in this molecule lies parallel to the *b*-inertial axis in the molecule (cf. Figure 7a).

Analysis of the most intense vibronic band of DBT (202 cm^{-1} above the origin band) shows that the active vibrational mode is the totally symmetric in-plane ring bending mode, similar to that observed in the CAR+210 and DBF+209 bands, since it is also a *b*-type band. The inertial defect values for this vibronic band also follow the trend exhibited by the corresponding bands of CAR and DBF. The $\Delta I'$ value decreases in magnitude from −0.73 to 0.00 uÅ^2, whereas the $\Delta I''$ value does not change (−0.74 uÅ^2) when going from the 0_0^0 to the +202 band in DBT (cf. Table 1). These observations are in excellent agreement with the theoretical results of Lee.[26]

The vibrationally resolved electronic spectra of DPF and DPO exhibit several low frequency band features (cf. Figure 4). Topp and co-workers[23] assigned the band at +66 cm^{-1} in DPO to an overtone (2 × 33 cm^{-1}) of the torsional motion of the phenyl groups with respect to the central ring. The band at +260 cm^{-1} has been assigned to a fundamental in-plane interannular bending motion in both molecules, whereas the group of lines at +876 cm^{-1} in DPF are strongly coupled, exhibit Franck−Condon progressions, and are assigned as an in-plane vibrational mode acting in the furan ring. We focus our attention on the zero point vibrational level (ZPL) transition of each molecule here.

From the fits of the rotationally resolved electronic spectra in Figures 5 and 6, we find that both molecules have long-axis polarized $S_1 \leftarrow S_0$ electronic transition moment vectors (cf. Figure 7b,c). The S_1 states of DPF and DPO are both ^1L_b states. This result indicates that the presence of the phenyl groups in the 2- and 5- positions of the central ring modifies the electronic distribution of the frontier molecular orbitals; hence, the S_1 states are different from that in DBF (^1L_a state).[20]

The calculated S_0 rotational constants of DPF and DPO are again in good agreement with the experimental values (see Table 1). Surprisingly, in these "more flexible" molecules, the changes in rotational constants upon excitation are all positive; $\Delta A = 6.8$, $\Delta B = 1.0$, and $\Delta C = 0.8$ MHz in DPF and $\Delta A = 10.2$, $\Delta B = 0.6$, and $\Delta C = 0.6$ MHz in DPO. Apparently, upon excitation, the molecules contract mainly in perpendicular directions with respect to their *a*-axes. Both molecules are essentially planar in both S_0 and S_1 states. DPF has an inertial defect value of 1.86 uÅ^2 in its S_0 state, a value that is consistent with a planar molecule having some in-plane degrees of freedom. However, by absorption of light, this value increases in magnitude to 3.22 uÅ^2, which highlights the floppiness of the molecule along certain in-plane torsional coordinates. DPO exhibits similar behavior in terms of inertial defect values, but these are somewhat larger in magnitude ($\Delta I'' = 3.35$ uÅ^2 and $\Delta I' = 4.10$ uÅ^2). Electronically excited-state calculations predict small changes within the central five-membered ring, due to the presence of the two extra nitrogen atoms in the structure.[21]

Dynamics. A remarkable observation in the fits of the high-resolution electronic spectra of DBT is the significant contribution of Lorentzian character to the Voigt line shape profiles, in contrast with that used in the fits of the corresponding spectra of FLU, CAR, and DBF. The vibronic bands DBT+202 and CAR+210 are compared in Figure 8. In DBT+202, a Lorentzian (natural) broadening of 195 MHz is required to properly fit the experimental trace, whereas, in CAR+210, the Lorentzian contribution in the Voigt profile is an order of magnitude less (18 MHz). Apparently, the presence of the heavy atom in the molecular structure contributes to the enhancement of the ISC dynamics by increasing the spin−orbit coupling terms (k_{st}) in

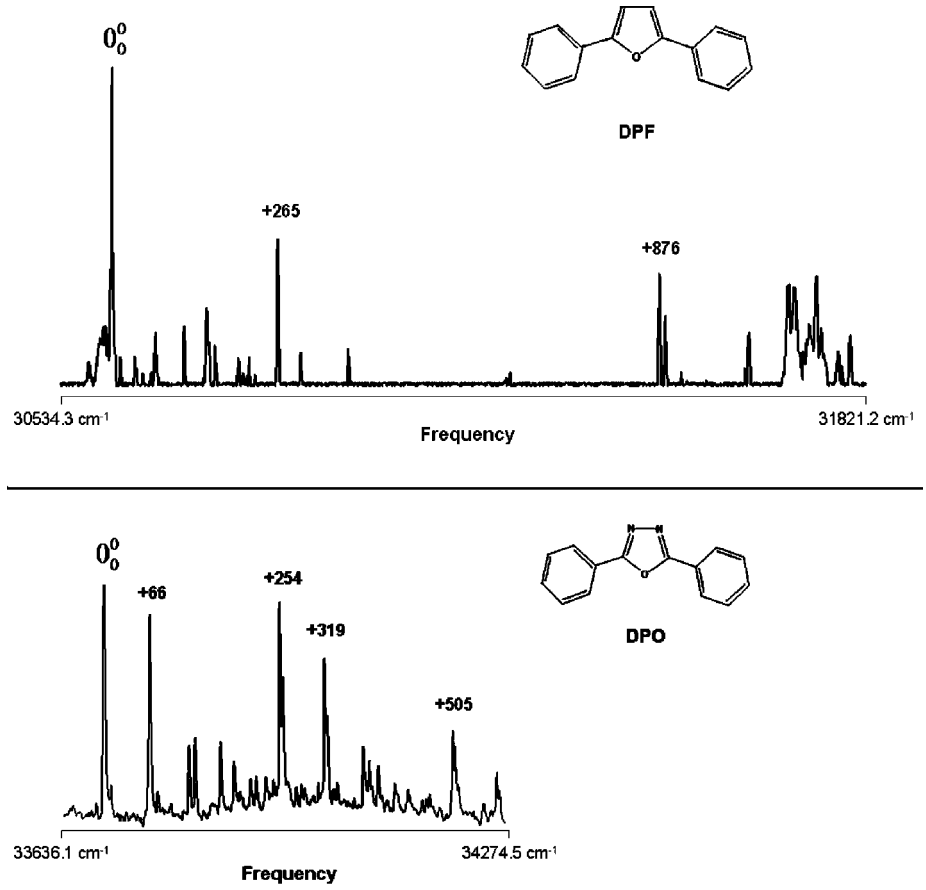

Figure 4. Vibrationally resolved fluorescence excitation spectra of DPF and DPO in the gas phase.

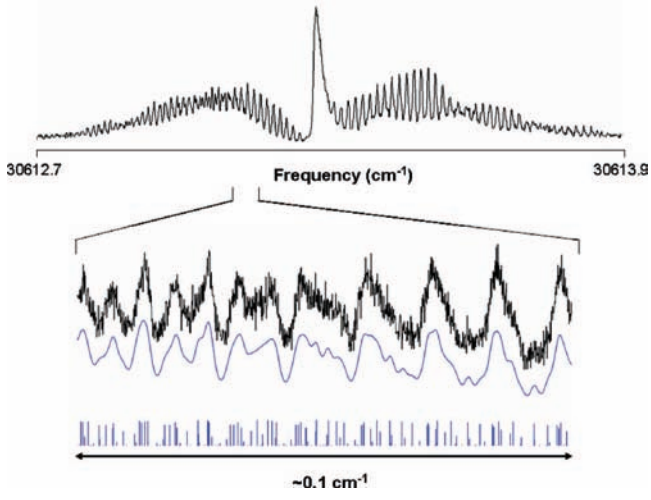

Figure 5. Rotationally resolved fluorescence excitation spectrum of the 0_0^0 band of DPF in the gas phase; the origin frequency is at 30613.3 cm^{-1}. A portion of the experimental trace and its corresponding simulated spectrum, with and without line shape functions, are also shown in the bottom panel.

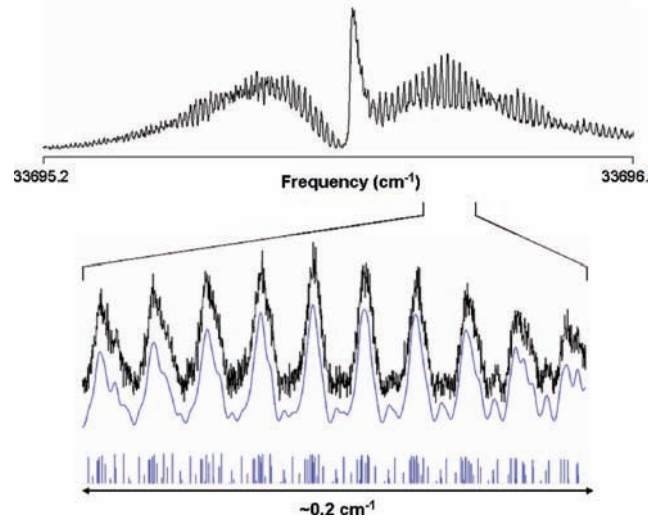

Figure 6. Rotationally resolved fluorescence excitation spectrum of the 0_0^0 band of DPO in the gas phase; the origin frequency is at 33695.9 cm^{-1}. A portion of the experimental trace and its corresponding simulation spectrum, with and without line shape functions, are also shown in the bottom panel.

the Hamiltonian and the density of dark states $\{|t\rangle\}$ available in the vicinity of the prepared singlet state $|s\rangle$.

Recent results for jet-cooled electronic spectroscopy experiments in the gas phase in the presence of magnetic fields (Zeeman effect)[27] show that the broadened rotational lines of DBT are insensitive to magnetic fields up to 1 T, in both the 0_0^0 (*b*-type) and the DBT+870 (*a*-type) bands (the latter is not shown in Figure 2d). This finding is expected for a system exhibiting ISC in the statistical limit, as the "prepared" eigenstates are already extensively mixed with the triplet levels in the electronically excited state.

In order to further investigate the ISC dynamics in this family of molecules (FLU-CAR-DBF-DBT), the fluorescence decay widths, FWHM, and γ_s (in MHz) have been summarized in Table 2 for each transition in every molecule analyzed. The corresponding fluorescence lifetimes τ_s (in ns) were computed by using the relationship between γ_s and τ_s, given by

$$\gamma_s = \frac{1}{2\pi\tau_s} \quad (1)$$

Interestingly, the largest τ_s value is observed in the 0_0^0 band of CAR. We also observe that vibrational motion decreases the lifetime in the S_1 state of the molecules, presumably by IVR along different low frequency coordinates, even though the vibronic bands show significant oscillator strengths. However, the most remarkable finding is the decrease of the fluorescence lifetime of DBT by a factor of ~10 with respect to that observed in FLU. This last observation is in good agreement with previous studies of the photophysical properties of several heterocycles in the condensed phase.[8,10]

As suggested in the classic paper of McClure,[28] analyses of the properties of aromatic polyatomic molecules containing heavy atoms require the consideration of spin−orbit coupling between their zero-order singlet and triplet states. Spin−orbit coupling (SOC) terms for isolated C, N, O and S atoms have been estimated.[28,29] As shown in Figure 9, the observed fluorescence lifetimes of DBT, DBF, and FLU are inversely proportional to the square root of these constants, $(SOC)^{1/2}$, in accord with expectations. The "anomalous" lifetime behavior of CAR might be due to a reduced unpaired electron spin density on the nitrogen atom in its S_1 state, since its lifetime is actually much longer than expected.

The two rotationally resolved electronic spectra of DPF and DPO also are unusual (see Figures 5 and 6). Even though the rotational temperature is fairly low (4 K) and the Doppler broadening of a single rotational transition is expected to be only 18 MHz, the spectra are significantly broader than this. Apparently, the ISC dynamics is enhanced by the presence of the heteroatoms in the central five-membered ring. Obukhov[11,14] has previously discussed these effects. There are many variations in the fluorescence properties of substituted five- or six-membered ring heterocycles due to the intramolecular interaction of nitrogen, oxygen, or sulfur atoms in 2-, 3-, 4- or 5-nonconcatenated chains. In condensed phase experiments, the excited-state lifetimes for DPF and DPO are reported to be ~0.4 ns.[14] The estimated excited-state lifetimes from our experiments in the gas phase are ~2.1 (1) ns for both molecules.

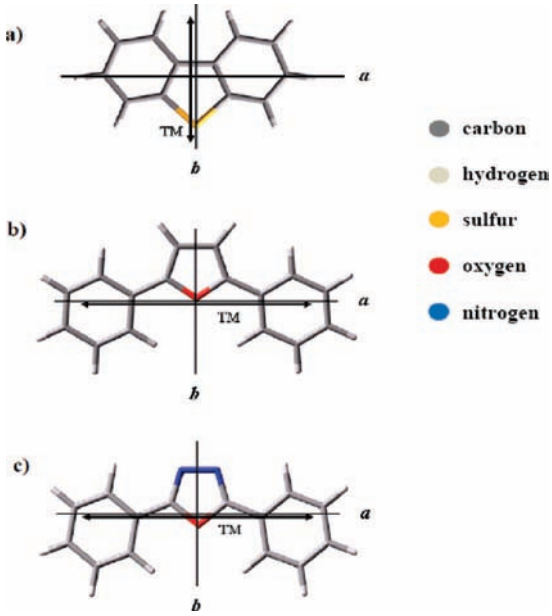

Figure 7. Electronic transition moment orientations of (a) DBT, (b) DPF, and (c) DPO.

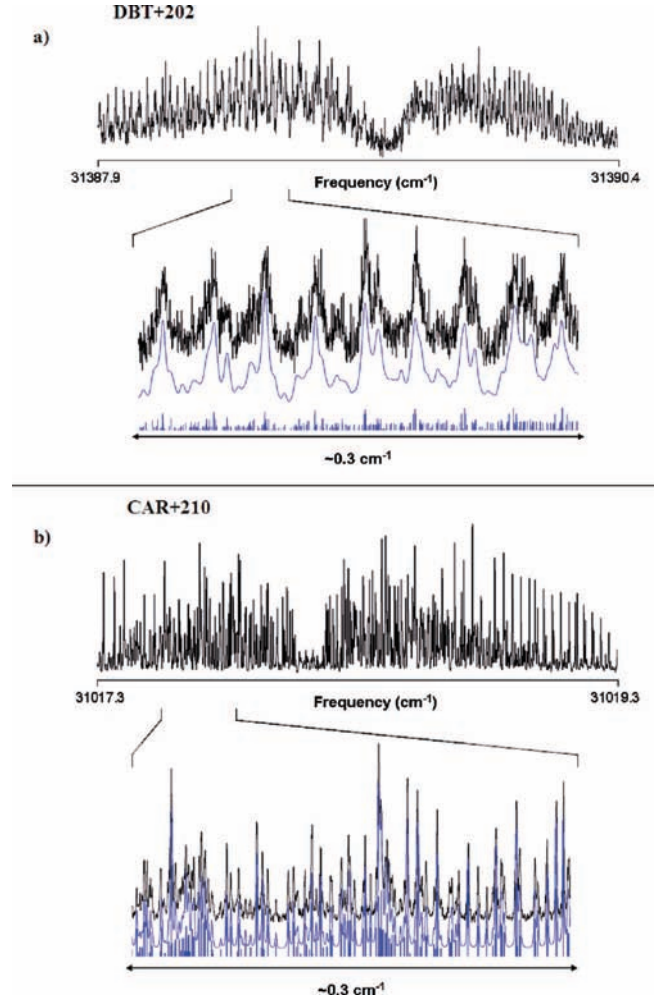

Figure 8. (a) Heavy atom effect in a vibronic band of dibenzothiophene (DBT+202) in the gas phase. A Lorentzian broadening of 195 MHz has been applied in the simulated trace. (b) The analogous transition of carbazole (CAR+210) is shown for comparison. The Lorentzian broadening of the fit is 18 MHz. The Gaussian (Doppler) broadening is 18 MHz in both spectra.

TABLE 2: Experimental Fluorescence Lifetime Broadenings and S_1 Lifetimes of Some Vibrational Bands of FLU, CAR, DBF and DBT from the Fits of Their High-Resolution Spectra in the Gas Phase[a,b]

band	fluorescence lifetime broadening, γ_s (MHz)	lifetime in the S_1 state, τ_s (ns)
FLU	15 (1)	10.6 (7)
FLU+204	24 (1)	6.6 (4)
FLU+394	30 (1)	5.3 (2)
CAR	11 (1)	14.5 (8)
CAR+210	18 (1)	8.8 (6)
CAR+511	23 (1)	6.9 (4)
DBF	21 (1)	7.6 (4)
DBF+209	31 (2)	5.1 (2)
DBF+443	27 (1)	5.9 (3)
DBT	167 (6)	1.0 (<1)
DBT+202	195 (6)	0.8 (<1)

[a] See Reference 20 for spectral details on the corresponding transitions of FLU, CAR, and DBF. [b] The standard deviations in the last significant figure are shown in parentheses.

Presumably, in DPF and DPO there is a high density of vibrational states due to the low-frequency torsional motion of the phenyl groups with respect to the central ring. In a separate publication, we have studied the effect of the low-frequency

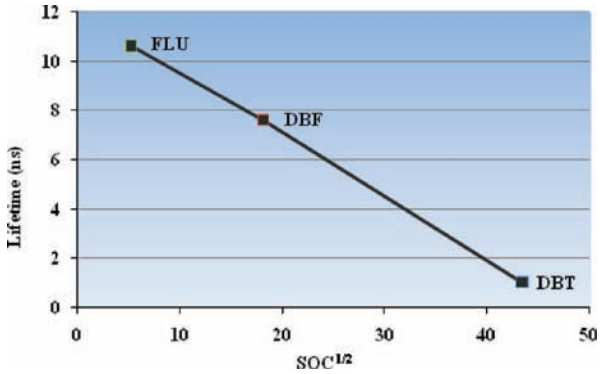

Figure 9. Plot of the fluorescence lifetimes vs the square root of the spin−orbit coupling terms of FLU, DBF, and DBT.

methyl group torsional levels on the ISC dynamics of two molecules containing a chromophore falling in the "intermediate" molecule limit; 2-methylpyrimidine and 5-methylpyrimidine.[30] In that work, we clearly observed the appearance of extra lines in the rotationally resolved electronic spectra, compared to what had been previously observed in pyrimidine itself.[31] Because furan and oxadiazole heterocycles fall in the statistical molecule limit, we believe that their corresponding phenyl derivatives, DPF and DPO, respectively, do not exhibit well-defined spectral signatures in the high-resolution spectra analyzed here.

It would be interesting to complement the present study with the analysis of some of the representative vibronic bands of these two molecules, and some other nonconcatenated polycycles with no heteroatoms present, such as *p*-terphenyl. This molecule is expected to exhibit ISC dynamics due to the presence of a low energy triplet state (T_β).[32]

5. Summary

Rotationally resolved $S_1 \leftarrow S_0$ fluorescence excitation spectra of the 0_0^0 bands of DBT, DPF, and DPO have been recorded in the collision-free environment of a molecular beam. Detailed analyses of these spectra make evident the existence of an ISC mechanism in the large molecule (statistical) limit upon excitation by UV light. DBT constitutes a special case in the family of FLU-CAR-DBF-DBT, since its excited-state lifetime (∼1 ns) is significantly shorter than those of the remaining molecules in this series. The observed lifetimes show an inverse correlation with the square root of the spin−orbit coupling constant of the attached "heavy atom". DPF and DPO also exhibit short excited-state lifetimes (∼2 ns), presumably due to the high density of dark-state energy levels in the vicinity of the prepared state.

Acknowledgment. L. Alvarez thanks Dr. M. Villanueva (University of Guanajuato, México) for his kind help with some of the theoretical calculations, whose results are presented here. This work has been supported by the NSF (CHE-0615755) to whom we are grateful.

References and Notes

(1) Robinson, G. W. *J. Chem. Phys.* **1967**, *47*, 1967.
(2) Atkins, P. W. Physical Chemistry, 6th ed.; W. H. Freeman and Co.: New York, 1998; pp 503−506.
(3) Bree, A.; Zwarich, R. *Spectrochim. Acta* **1971**, *27A*, 599.
(4) Bree, A.; Zwarich, R. *Spectrochim. Acta* **1971**, *27A*, 621.
(5) Castellucci, E.; Foggi, P.; Salvi, P. R. *Chem. Phys.* **1981**, *63*, 437.
(6) Yamaguchi, H.; Higashi, M. *Spectrochim. Acta* **1987**, *43A*, 1431.
(7) Spanget-Larsen, J.; Thulstrup, E. W. *J. Mol. Struct.* **2003**, *661−662*, 603.
(8) Zander, M.; Kirsch, G. *Z. Naturforsch.* **1989**, *44A*, 205.
(9) Wang, X.; Tian, J.; Kofron, W. G.; Lim, E. C. *J. Phys. Chem.* **1999**, *103A*, 1560.
(10) Nijegorodov, N.; Luhanga, P. V. C.; Nkoma, J. S.; Winkoun, D. P. *Spectrochim. Acta* **2006**, *64A*, 1, and references therein.
(11) Obukhov, A. E. *Laser Phys.* **2003**, *13*, 847.
(12) Kamiya, M. *Bull. Chem. Soc. Jpn.* **1970**, *43*, 3344.
(13) Abakumov, G. A.; Drobakha, S. A.; Klimanov, A. V.; Ostrovskii, A. V.; Polyakov, B. I.; Simonov, A. P. *Kvantovaya Elektron* **1986**, *13*, 2364.
(14) Obukhov, A. E. *Laser Phys.* **1999**, *9*, 699.
(15) Luňák, S., Jr.; Nepră, M.; Hrdina, R.; Kurfürst, A.; Kuthan, J. *Chem. Phys.* **1993**, *170*, 77.
(16) Majewski, W. A.; Pfanstiel, J. F.; Plusquellic, D. F.; Pratt, D. W. *Laser Techniques in Chemistry*; Rizzo, T. R., Myers, A. B., Eds.; J. Wiley & Sons: New York, 1995; pp 101.
(17) Leutwyler, S.; Even, U.; Jortner, J. *Chem. Phys. Lett.* **1982**, *86*, 439.
(18) Auty, A. R.; Jones, A. C.; Phillips, D. *J. Chem. Soc., Faraday Trans. 2* **1986**, *82*, 1219.
(19) Chakraborty, T.; Lim, E. C. *Chem. Phys. Lett.* **1993**, *207*, 99.
(20) Yi, J. T.; Alvarez-Valtierra, L.; Pratt, D. W. *J. Chem. Phys.* **2006**, *124*, 244302.
(21) Frisch, M. J.; Trucks, G. W.; Schlegel, H. B.; Scuseria, G. E.; Robb, M. A.; Cheeseman, J. R.; Montgomery, J. A., Jr.; Vreven, T.; Kudin, K. N.; Burant, J. C.; Millam, J. M.; Iyengar, S. S.; Tomasi, J.; Barone, V.; Mennucci, B.; Cossi, M.; Scalmani, G.; Rega, N.; Petersson, G. A.; Nakatsuji, H.; Hada, M.; Ehara, M.; Toyota, K.; Fukuda, R.; Hasegawa, J.; Ishida, M.; Nakajima, T.; Honda, Y.; Kitao, O.; Nakai, H.; Klene, M.; Li, X.; Knox, J. E.; Hratchian, H. P.; Cross, J. B.; Bakken, V.; Adamo, C.; Jaramillo, J.; Gomperts, R.; Stratmann, R. E.; Yazyev, O.; Austin, A. J.; Cammi, R.; Pomelli, C.; Ochterski, J. W.; Ayala, P. Y.; Morokuma, K.; Voth, G. A.; Salvador, P.; Dannenberg, J. J.; Zakrzewski, V. G.; Dapprich, S.; Daniels, A. D.; Strain, M. C.; Farkas, O.; Malick, D. K.; Rabuck, A. D.; Raghavachari, K.; Foresman, J. B.; Ortiz, J. V.; Cui, Q.; Baboul, A. G.; Clifford, S.; Cioslowski, J.; Stefanov, B. B.; Liu, G.; Liashenko, A.; Piskorz, P.; Komaromi, I.; Martin, R. L.; Fox, D. J.; Keith, T.; Al-Laham, M. A.; Peng, C. Y.; Nanayakkara, A.; Challacombe, M.; Gill, P. M. W.; Johnson, B.; Chen, W.; Wong, M. W.; Gonzalez, C.; Pople, J. A. *Gaussian 03, Revision C.02*; Gaussian, Inc.: Wallingford, CT, 2004.
(22) Plusquellic, D. F. *JB95 Spectral Fitting Program*; NIST: Gaithersburg, MD. http://physics.nist.gov/jb95.
(23) Mangle, E. A.; Salvi, P. R.; Babbit, R. J.; Motyka, A. L.; Topp, M. R. *Chem. Phys. Lett.* **1987**, *133*, 214.
(24) Roebber, J. L.; Gerrity, D. P.; Hemley, R.; Vaida, V. *Chem. Phys. Lett.* **1980**, *75*, 104.
(25) Platt, J. R. *J. Chem. Phys.* **1951**, *19*, 101.
(26) Lee, S. Y. *J. Phys. Chem.* **2001**, *105A*, 8093.
(27) Baba, M. Private communication, 2008.
(28) McClure, D. S. *J. Chem. Phys.* **1952**, *20*, 682.
(29) Gastilovich, E. A.; Serov, S. A.; Klimemko, V. G.; Korol'kova, N. V.; Nurmukhametov, R. N. *Mol. Spectrosc.* **2005**, *99*, 897.
(30) Alvarez-Valtierra, L.; Tan, X.-Q.; Pratt, D. W. *J. Phys. Chem.* **2007**, *111A*, 12802.
(31) Konings, J. A.; Majewski, W. A.; Matsumoto, Y.; Pratt, D. W.; Meerts, W. L. *J. Chem. Phys.* **1988**, *89*, 1813.
(32) Nijegorodov, N.; Winkoun, D. P.; Nkoma, J. S. *Spectrochim. Acta* **2004**, *60A*, 2035.

JP807397T